Study of charmless decays $B^{\pm} \to K^0_s K^0_s h^{\pm}$ ($h = K, \pi$) at Belle

A. Abdesselam,[101] I. Adachi,[22,18] K. Adamczyk,[75] J. K. Ahn,[50] H. Aihara,[109] S. Al Said,[101,47] K. Arinstein,[5,79] Y. Arita,[67] D. M. Asner,[4] H. Atmacan,[97] V. Aulchenko,[5,79] T. Aushev,[66] R. Ayad,[101] T. Aziz,[102] V. Babu,[102] I. Badhrees,[101,46] S. Bahinipati,[29] A. M. Bakich,[100] Y. Ban,[84] V. Bansal,[82] E. Barberio,[62] M. Barrett,[115] W. Bartel,[10] P. Behera,[32] C. Beleño,[17] K. Belous,[36] M. Berger,[98] F. Bernlochner,[3] D. Besson,[65] V. Bhardwaj,[28] B. Bhuyan,[30] T. Bilka,[6] J. Biswal,[41] T. Bloomfield,[62] A. Bobrov,[5,79] A. Bondar,[5,79] G. Bonvicini,[115] A. Bozek,[75] M. Bračko,[60,41] N. Braun,[43] F. Breibeck,[35] J. Brodzicka,[75] T. E. Browder,[21] L. Cao,[43] G. Caria,[62] D. Červenkov,[6] M.-C. Chang,[13] P. Chang,[74] Y. Chao,[74] V. Chekelian,[61] A. Chen,[72] K.-F. Chen,[74] B. G. Cheon,[20] K. Chilikin,[55] R. Chistov,[55,65] K. Cho,[49] V. Chobanova,[61] S.-K. Choi,[19] Y. Choi,[99] S. Choudhury,[31] D. Cinabro,[115] J. Crnkovic,[27] S. Cunliffe,[10] T. Czank,[107] M. Danilov,[65,55] N. Dash,[29] S. Di Carlo,[53] J. Dingfelder,[3] Z. Doležal,[6] T. V. Dong,[22,18] D. Dossett,[62] Z. Drásal,[6] A. Drutskoy,[55,65] S. Dubey,[21] D. Dutta,[102] S. Eidelman,[5,79] D. Epifanov,[5,79] J. E. Fast,[82] M. Feindt,[43] T. Ferber,[10] A. Frey,[17] O. Frost,[10] B. G. Fulsom,[82] R. Garg,[83] V. Gaur,[102] N. Gabyshev,[5,79] A. Garmash,[5,79] M. Gelb,[43] J. Gemmler,[43] D. Getzkow,[15] F. Giordano,[27] A. Giri,[31] R. Glattauer,[35] Y. M. Goh,[20] P. Goldenzweig,[43] B. Golob,[56,41] D. Greenwald,[104] M. Grosse Perdekamp,[27,90] J. Grygier,[43] O. Grzymkowska,[75] Y. Guan,[33,22] E. Guido,[39] H. Guo,[92] J. Haba,[22,18] P. Hamer,[17] K. Hara,[22] T. Hara,[22,18] Y. Hasegawa,[94] J. Hasenbusch,[3] K. Hayasaka,[77] H. Hayashii,[71] X. H. He,[84] M. Heck,[43] M. T. Hedges,[21] D. Heffernan,[81] M. Heider,[43] A. Heller,[43] T. Higuchi,[44] S. Hirose,[67] T. Horiguchi,[107] Y. Hoshi,[106] K. Hoshina,[112] W.-S. Hou,[74] Y. B. Hsiung,[74] C.-L. Hsu,[100] K. Huang,[74] M. Huschle,[43] Y. Igarashi,[22] T. Iijima,[68,67] M. Imamura,[67] K. Inami,[67] G. Inguglia,[10] A. Ishikawa,[107] K. Itagaki,[107] R. Itoh,[22,18] M. Iwasaki,[80] Y. Iwasaki,[22] S. Iwata,[111] W. W. Jacobs,[33] I. Jaegle,[12] H. B. Jeon,[52] S. Jia,[2] Y. Jin,[109] D. Joffe,[45] M. Jones,[21] K. K. Joo,[8] T. Julius,[62] J. Kahn,[57] H. Kakuno,[111] A. B. Kaliyar,[32] J. H. Kang,[117] K. H. Kang,[52] P. Kapusta,[75] G. Karyan,[10] S. U. Kataoka,[70] E. Kato,[107] Y. Kato,[67] P. Katrenko,[66,55] H. Kawai,[7] T. Kawasaki,[77] T. Keck,[43] H. Kichimi,[22] C. Kiesling,[61] B. H. Kim,[93] D. Y. Kim,[96] H. J. Kim,[52] H.-J. Kim,[117] J. B. Kim,[50] K. T. Kim,[50] S. H. Kim,[20] S. K. Kim,[93] Y. J. Kim,[50] T. Kimmel,[114] H. Kindo,[22,18] K. Kinoshita,[9] C. Kleinwort,[10] J. Klucar,[41] N. Kobayashi,[110] P. Kodyš,[6] Y. Koga,[67] T. Konno,[48] S. Korpar,[60,41] D. Kotchetkov,[21] R. T. Kouzes,[82] P. Križan,[56,41] R. Kroeger,[63] J.-F. Krohn,[62] P. Krokovny,[5,79] B. Kronenbitter,[43] T. Kuhr,[57] R. Kulasiri,[45] R. Kumar,[86] T. Kumita,[111] E. Kurihara,[7] Y. Kuroki,[81] A. Kuzmin,[5,79] P. Kvasnička,[6] Y.-J. Kwon,[117] Y.-T. Lai,[22] J. S. Lange,[15] I. S. Lee,[20] S. C. Lee,[52] M. Leitgab,[27,90] R. Leitner,[6] D. Levit,[104] P. Lewis,[21] C. H. Li,[62] H. Li,[33] L. K. Li,[34] Y. Li,[114] Y. B. Li,[84] L. Li Gioi,[61] J. Libby,[32] A. Limosani,[62] Z. Liptak,[21] C. Liu,[92] Y. Liu,[9] D. Liventsev,[114,22] A. Loos,[97] R. Louvot,[54] P.-C. Lu,[74] M. Lubej,[41] T. Luo,[14] J. MacNaughton,[64] M. Masuda,[108] T. Matsuda,[64] D. Matvienko,[5,79] A. Matyja,[75] J. T. McNeil,[12] M. Merola,[38,69] F. Metzner,[43] Y. Mikami,[107] K. Miyabayashi,[71] Y. Miyachi,[116] H. Miyake,[22,18] H. Miyata,[77] Y. Miyazaki,[67]

R. Mizuk,[55,65,66] G. B. Mohanty,[102] S. Mohanty,[102,113] H. K. Moon,[50] T. Mori,[67] T. Morii,[44] H.-G. Moser,[61] M. Mrvar,[41] T. Müller,[43] N. Muramatsu,[87] R. Mussa,[39] Y. Nagasaka,[25] Y. Nakahama,[109] I. Nakamura,[22,18] K. R. Nakamura,[22] E. Nakano,[80] H. Nakano,[107] T. Nakano,[88] M. Nakao,[22,18] H. Nakayama,[22,18] H. Nakazawa,[74] T. Nanut,[41] K. J. Nath,[30] Z. Natkaniec,[75] M. Nayak,[115,22] K. Neichi,[106] C. Ng,[109] C. Niebuhr,[10] M. Niiyama,[51] N. K. Nisar,[85] S. Nishida,[22,18] K. Nishimura,[21] O. Nitoh,[112] A. Ogawa,[90] K. Ogawa,[77] S. Ogawa,[105] T. Ohshima,[67] S. Okuno,[42] S. L. Olsen,[19] H. Ono,[76,77] Y. Ono,[107] Y. Onuki,[109] W. Ostrowicz,[75] C. Oswald,[3] H. Ozaki,[22,18] P. Pakhlov,[55,65] G. Pakhlova,[55,66] B. Pal,[4] H. Palka,[75] E. Panzenböck,[17,71] S. Pardi,[38] C.-S. Park,[117] C. W. Park,[99] H. Park,[52] K. S. Park,[99] S. Paul,[104] I. Pavelkin,[66] T. K. Pedlar,[58] T. Peng,[92] L. Pesántez,[3] R. Pestotnik,[41] M. Peters,[21] L. E. Piilonen,[114] A. Poluektov,[5,79] V. Popov,[55,66] K. Prasanth,[102] E. Prencipe,[24] M. Prim,[43] K. Prothmann,[61,103] M. V. Purohit,[97] A. Rabusov,[104] J. Rauch,[104] B. Reisert,[61] P. K. Resmi,[32] E. Ribežl,[41] M. Ritter,[57] J. Rorie,[21] A. Rostomyan,[10] M. Rozanska,[75] S. Rummel,[57] G. Russo,[38] D. Sahoo,[102] H. Sahoo,[63] T. Saito,[107] Y. Sakai,[22,18] M. Salehi,[59,57] S. Sandilya,[9] D. Santel,[9] L. Santelj,[22] T. Sanuki,[107] J. Sasaki,[109] N. Sasao,[51] Y. Sato,[67] V. Savinov,[85] T. Schlüter,[57] O. Schneider,[54] G. Schnell,[1,26] P. Schönmeier,[107] M. Schram,[82] J. Schueler,[21] C. Schwanda,[35] A. J. Schwartz,[9] B. Schwenker,[17] R. Seidl,[90] Y. Seino,[77] D. Semmler,[15] K. Senyo,[116] O. Seon,[67] I. S. Seong,[21] M. E. Sevior,[62] L. Shang,[34] M. Shapkin,[36] V. Shebalin,[5,79] C. P. Shen,[2] T.-A. Shibata,[110] H. Shibuya,[105] S. Shinomiya,[81] J.-G. Shiu,[74] B. Shwartz,[5,79] A. Sibidanov,[100] F. Simon,[61,103] J. B. Singh,[83] R. Sinha,[37] A. Sokolov,[36] Y. Soloviev,[10] E. Solovieva,[55,66] S. Stanič,[78] M. Starič,[41] M. Steder,[10] Z. Stottler,[114] J. F. Strube,[82] J. Stypula,[75] S. Sugihara,[109] A. Sugiyama,[91] M. Sumihama,[16] K. Sumisawa,[22,18] T. Sumiyoshi,[111] W. Sutcliffe,[43] K. Suzuki,[67] K. Suzuki,[98] S. Suzuki,[91] S. Y. Suzuki,[22] Z. Suzuki,[107] H. Takeichi,[67] M. Takizawa,[95,23,89] U. Tamponi,[39] M. Tanaka,[22,18] S. Tanaka,[22,18] K. Tanida,[40] N. Taniguchi,[22] Y. Tao,[12] G. N. Taylor,[62] F. Tenchini,[62] Y. Teramoto,[80] I. Tikhomirov,[65] K. Trabelsi,[22,18] T. Tsuboyama,[22,18] M. Uchida,[110] T. Uchida,[22] I. Ueda,[22] S. Uehara,[22,18] T. Uglov,[55,66] Y. Unno,[20] S. Uno,[22,18] P. Urquijo,[62] Y. Ushiroda,[22,18] Y. Usov,[5,79] S. E. Vahsen,[21] R. Van Tonder,[43] C. Van Hulse,[1] P. Vanhoefer,[61] G. Varner,[21] K. E. Varvell,[100] K. Vervink,[54] A. Vinokurova,[5,79] V. Vorobyev,[5,79] A. Vossen,[11] M. N. Wagner,[15] E. Waheed,[62] B. Wang,[9] C. H. Wang,[73] M.-Z. Wang,[74] P. Wang,[34] X. L. Wang,[14] M. Watanabe,[77] Y. Watanabe,[42] S. Watanuki,[107] R. Wedd,[62] S. Wehle,[10] E. Widmann,[98] J. Wiechczynski,[75] K. M. Williams,[114] E. Won,[50] B. D. Yabsley,[100] S. Yamada,[22] H. Yamamoto,[107] Y. Yamashita,[76] S. Yashchenko,[10] H. Ye,[10] J. Yelton,[12] J. H. Yin,[34] Y. Yook,[117] C. Z. Yuan,[34] Y. Yusa,[77] S. Zakharov,[55,66] C. C. Zhang,[34] L. M. Zhang,[92] Z. P. Zhang,[92] L. Zhao,[92] V. Zhilich,[5,79] V. Zhukova,[55,65] V. Zhulanov,[5,79] T. Zivko,[41] A. Zupanc,[56,41] and N. Zwahlen[54]

(The Belle Collaboration)

[1]*University of the Basque Country UPV/EHU, 48080 Bilbao*
[2]*Beihang University, Beijing 100191*
[3]*University of Bonn, 53115 Bonn*
[4]*Brookhaven National Laboratory, Upton, New York 11973*
[5]*Budker Institute of Nuclear Physics SB RAS, Novosibirsk 630090*
[6]*Faculty of Mathematics and Physics, Charles University, 121 16 Prague*

[7]*Chiba University, Chiba 263-8522*
[8]*Chonnam National University, Kwangju 660-701*
[9]*University of Cincinnati, Cincinnati, Ohio 45221*
[10]*Deutsches Elektronen–Synchrotron, 22607 Hamburg*
[11]*Duke University, Durham, North Carolina 27708*
[12]*University of Florida, Gainesville, Florida 32611*
[13]*Department of Physics, Fu Jen Catholic University, Taipei 24205*
[14]*Key Laboratory of Nuclear Physics and Ion-beam Application (MOE) and Institute of Modern Physics, Fudan University, Shanghai 200443*
[15]*Justus-Liebig-Universität Gießen, 35392 Gießen*
[16]*Gifu University, Gifu 501-1193*
[17]*II. Physikalisches Institut, Georg-August-Universität Göttingen, 37073 Göttingen*
[18]*SOKENDAI (The Graduate University for Advanced Studies), Hayama 240-0193*
[19]*Gyeongsang National University, Chinju 660-701*
[20]*Hanyang University, Seoul 133-791*
[21]*University of Hawaii, Honolulu, Hawaii 96822*
[22]*High Energy Accelerator Research Organization (KEK), Tsukuba 305-0801*
[23]*J-PARC Branch, KEK Theory Center, High Energy Accelerator Research Organization (KEK), Tsukuba 305-0801*
[24]*Forschungszentrum Jülich, 52425 Jülich*
[25]*Hiroshima Institute of Technology, Hiroshima 731-5193*
[26]*IKERBASQUE, Basque Foundation for Science, 48013 Bilbao*
[27]*University of Illinois at Urbana-Champaign, Urbana, Illinois 61801*
[28]*Indian Institute of Science Education and Research Mohali, SAS Nagar, 140306*
[29]*Indian Institute of Technology Bhubaneswar, Satya Nagar 751007*
[30]*Indian Institute of Technology Guwahati, Assam 781039*
[31]*Indian Institute of Technology Hyderabad, Telangana 502285*
[32]*Indian Institute of Technology Madras, Chennai 600036*
[33]*Indiana University, Bloomington, Indiana 47408*
[34]*Institute of High Energy Physics, Chinese Academy of Sciences, Beijing 100049*
[35]*Institute of High Energy Physics, Vienna 1050*
[36]*Institute for High Energy Physics, Protvino 142281*
[37]*Institute of Mathematical Sciences, Chennai 600113*
[38]*INFN - Sezione di Napoli, 80126 Napoli*
[39]*INFN - Sezione di Torino, 10125 Torino*
[40]*Advanced Science Research Center, Japan Atomic Energy Agency, Naka 319-1195*
[41]*J. Stefan Institute, 1000 Ljubljana*
[42]*Kanagawa University, Yokohama 221-8686*
[43]*Institut für Experimentelle Teilchenphysik, Karlsruher Institut für Technologie, 76131 Karlsruhe*
[44]*Kavli Institute for the Physics and Mathematics of the Universe (WPI), University of Tokyo, Kashiwa 277-8583*
[45]*Kennesaw State University, Kennesaw, Georgia 30144*
[46]*King Abdulaziz City for Science and Technology, Riyadh 11442*

[47]*Department of Physics, Faculty of Science, King Abdulaziz University, Jeddah 21589*
[48]*Kitasato University, Tokyo 108-0072*
[49]*Korea Institute of Science and Technology Information, Daejeon 305-806*
[50]*Korea University, Seoul 136-713*
[51]*Kyoto University, Kyoto 606-8502*
[52]*Kyungpook National University, Daegu 702-701*
[53]*LAL, Univ. Paris-Sud, CNRS/IN2P3, Université Paris-Saclay, Orsay*
[54]*École Polytechnique Fédérale de Lausanne (EPFL), Lausanne 1015*
[55]*P.N. Lebedev Physical Institute of the Russian Academy of Sciences, Moscow 119991*
[56]*Faculty of Mathematics and Physics, University of Ljubljana, 1000 Ljubljana*
[57]*Ludwig Maximilians University, 80539 Munich*
[58]*Luther College, Decorah, Iowa 52101*
[59]*University of Malaya, 50603 Kuala Lumpur*
[60]*University of Maribor, 2000 Maribor*
[61]*Max-Planck-Institut für Physik, 80805 München*
[62]*School of Physics, University of Melbourne, Victoria 3010*
[63]*University of Mississippi, University, Mississippi 38677*
[64]*University of Miyazaki, Miyazaki 889-2192*
[65]*Moscow Physical Engineering Institute, Moscow 115409*
[66]*Moscow Institute of Physics and Technology, Moscow Region 141700*
[67]*Graduate School of Science, Nagoya University, Nagoya 464-8602*
[68]*Kobayashi-Maskawa Institute, Nagoya University, Nagoya 464-8602*
[69]*Università di Napoli Federico II, 80055 Napoli*
[70]*Nara University of Education, Nara 630-8528*
[71]*Nara Women's University, Nara 630-8506*
[72]*National Central University, Chung-li 32054*
[73]*National United University, Miao Li 36003*
[74]*Department of Physics, National Taiwan University, Taipei 10617*
[75]*H. Niewodniczanski Institute of Nuclear Physics, Krakow 31-342*
[76]*Nippon Dental University, Niigata 951-8580*
[77]*Niigata University, Niigata 950-2181*
[78]*University of Nova Gorica, 5000 Nova Gorica*
[79]*Novosibirsk State University, Novosibirsk 630090*
[80]*Osaka City University, Osaka 558-8585*
[81]*Osaka University, Osaka 565-0871*
[82]*Pacific Northwest National Laboratory, Richland, Washington 99352*
[83]*Panjab University, Chandigarh 160014*
[84]*Peking University, Beijing 100871*
[85]*University of Pittsburgh, Pittsburgh, Pennsylvania 15260*
[86]*Punjab Agricultural University, Ludhiana 141004*
[87]*Research Center for Electron Photon Science, Tohoku University, Sendai 980-8578*
[88]*Research Center for Nuclear Physics, Osaka University, Osaka 567-0047*
[89]*Theoretical Research Division, Nishina Center, RIKEN, Saitama 351-0198*
[90]*RIKEN BNL Research Center, Upton, New York 11973*

[91] Saga University, Saga 840-8502
[92] University of Science and Technology of China, Hefei 230026
[93] Seoul National University, Seoul 151-742
[94] Shinshu University, Nagano 390-8621
[95] Showa Pharmaceutical University, Tokyo 194-8543
[96] Soongsil University, Seoul 156-743
[97] University of South Carolina, Columbia, South Carolina 29208
[98] Stefan Meyer Institute for Subatomic Physics, Vienna 1090
[99] Sungkyunkwan University, Suwon 440-746
[100] School of Physics, University of Sydney, New South Wales 2006
[101] Department of Physics, Faculty of Science, University of Tabuk, Tabuk 71451
[102] Tata Institute of Fundamental Research, Mumbai 400005
[103] Excellence Cluster Universe, Technische Universität München, 85748 Garching
[104] Department of Physics, Technische Universität München, 85748 Garching
[105] Toho University, Funabashi 274-8510
[106] Tohoku Gakuin University, Tagajo 985-8537
[107] Department of Physics, Tohoku University, Sendai 980-8578
[108] Earthquake Research Institute, University of Tokyo, Tokyo 113-0032
[109] Department of Physics, University of Tokyo, Tokyo 113-0033
[110] Tokyo Institute of Technology, Tokyo 152-8550
[111] Tokyo Metropolitan University, Tokyo 192-0397
[112] Tokyo University of Agriculture and Technology, Tokyo 184-8588
[113] Utkal University, Bhubaneswar 751004
[114] Virginia Polytechnic Institute and State University, Blacksburg, Virginia 24061
[115] Wayne State University, Detroit, Michigan 48202
[116] Yamagata University, Yamagata 990-8560
[117] Yonsei University, Seoul 120-749

Abstract

We report a search for charmless hadronic decays of charged B mesons to the final states $K^0_S K^0_S K^\pm$ and $K^0_S K^0_S \pi^\pm$. The results are based on a 711 fb^{-1} data sample that contains 772×10^6 $B\overline{B}$ pairs, and was collected at the $\Upsilon(4S)$ resonance with the Belle detector at the KEKB asymmetric-energy e^+e^- collider. For $B^\pm \to K^0_S K^0_S K^\pm$ decays, the measured branching fraction and direct CP asymmetry are $[10.64 \pm 0.49(\text{stat}) \pm 0.44(\text{syst})] \times 10^{-6}$ and $[-0.6 \pm 3.9(\text{stat}) \pm 3.4(\text{syst})]\%$, respectively. In the absence of a statistically significant signal for $B^\pm \to K^0_S K^0_S \pi^\pm$, we set the 90% confidence-level upper limit on its branching fraction at 1.14×10^{-6}.

Charged B-meson decays to three-body charmless hadronic final states $K^0_S K^0_S K^\pm$ and $K^0_S K^0_S \pi^\pm$ mainly proceed via the $\overline{b} \to \overline{s}$ and $\overline{b} \to \overline{d}$ loop transitions, respectively. Figure 1 shows the dominant Feynman diagrams that contribute to the decays. These are flavour changing neutral current transitions, which are suppressed in the standard model (SM) and hence provide a good avenue to search for physics beyond the SM [1]. Further motivation, especially to study the contributions of various quasi-two-body resonances to inclusive *CP* asymmetry, comes from the recent results on $B^\pm \to K^+K^-K^\pm$, $K^+K^-\pi^\pm$ and other such three-body decays [2–4]. LHCb has found large inclusive asymmetries in $B^\pm \to K^+K^-\pi^\pm$ and $\pi^+\pi^-\pi^\pm$ decays [3], where the observed phenomena are largely in localized regions of phase space. Recently, Belle has also reported strong evidence for a large *CP* asymmetry in the low K^+K^- invariant-mass region of $B^\pm \to K^+K^-\pi^\pm$ [4].

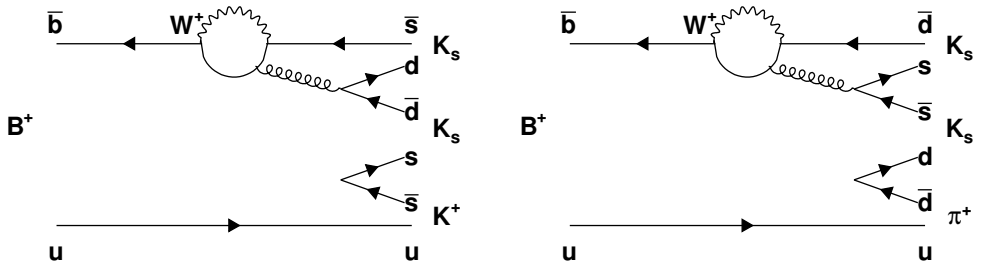

FIG. 1: Dominant Feynman diagrams that contribute to the decays $B^\pm \to K^0_S K^0_S K^\pm$ (left) and $B^\pm \to K^0_S K^0_S \pi^\pm$ (right).

The three-body decay $B^+ \to K^0_S K^0_S K^+$ [5] has already been observed and subsequently studied by the Belle and BaBar Collaborations [6–8]. Belle measured its branching fraction as $(13.4 \pm 1.9 \pm 1.5) \times 10^{-6}$ based on a small data set of $70\,\text{fb}^{-1}$ [7], while BaBar reported a branching fraction of $(10.6 \pm 0.5 \pm 0.3) \times 10^{-6}$ and an inclusive *CP* asymmetry of $(4^{+4}_{-5} \pm 2)\%$ using $426\,\text{fb}^{-1}$ of data [6]. The quoted uncertainties are statistical and systematic, respectively. On the other hand, the decay $B^+ \to K^0_S K^0_S \pi^+$ has not yet been observed, with the most restrictive upper limit being available at 90 % confidence level, $\mathcal{B}(B^+ \to K^0_S K^0_S \pi^+) < 5.1 \times 10^{-7}$, from BaBar [8].

We present herein an improved measurement of the branching fraction and direct *CP* asymmetry of the decay $B^+ \to K^0_S K^0_S K^+$ as well as a search for the decay $B^+ \to K^0_S K^0_S \pi^+$ based on the full $\Upsilon(4S)$ data sample, containing 772×10^6 $B\overline{B}$ pairs, collected with the Belle detector [9] at the KEKB asymmetric-energy e^+e^- (3.5 on 8.0 GeV) collider [10]. The direct *CP* asymmetry in the former case is given by

$$\mathcal{A}_{CP} = \frac{N(B^- \to K^0_S K^0_S K^-) - N(B^+ \to K^0_S K^0_S K^+)}{N(B^- \to K^0_S K^0_S K^-) + N(B^+ \to K^0_S K^0_S K^+)}, \tag{1}$$

where N is the signal yield obtained for the corresponding mode. The principal detector components used in the study are: a silicon vertex detector, a 50-layer central drift chamber (CDC), an array of aerogel threshold Cherenkov counters (ACC), a barrel-like arrangement of time-of-flight scintillation counters (TOF), and a CsI(Tl) crystal electromagnetic calorimeter (ECL). All these components are located inside a 1.5 T solenoidal magnetic field.

To reconstruct $B^+ \to K^0_S K^0_S h^+$ decay candidates, we combine a pair of K^0_S mesons with a charged kaon or pion. Each charged track candidate must have a distance of closest

approach with respect to the interaction point (IP) of less than 0.2 cm in the transverse r–ϕ plane and less than 5.0 cm along the z axis. Here, the z axis is the direction opposite the e^+ beam. Charged kaons and pions are identified based on a likelihood ratio $\mathcal{R}_{K/\pi} = \mathcal{L}_K/(\mathcal{L}_K + \mathcal{L}_\pi)$, where $\mathcal{L}_K$ and $\mathcal{L}_\pi$ denote the individual likelihood for kaons and pions, respectively, calculated using specific ionization in the CDC and information from the ACC and the TOF. A requirement, $\mathcal{R}_{K/\pi} > 0.6$, is applied to select the kaon candidates; track candidates failing it are classified as pions. The efficiency for kaon (pion) identification is 86% (91%) with a pion (kaon) misidentification rate of about 14% (9%).

The K^0_S candidates are reconstructed from pairs of oppositely charged tracks, both treated as pions, and are identified with a neural network (NN) [11]. The NN uses the following seven input variables: the K^0_S momentum in the laboratory frame, the distance along the z axis between the two track helices at their closest approach, the K^0_S flight length in the transverse plane, the angle between the K^0_S momentum and the vector joining the IP to the K^0_S decay vertex, the angle between the pion momentum and the laboratory frame direction in the K^0_S rest frame, the distances of closest approach in the transverse plane between the IP and the two pion helices, and the total number of hits (in the CDC and SVD) for each pion track. We also require that the reconstructed invariant mass be between 491 and 505 MeV/c^2, corresponding to $\pm 3\sigma$ around the nominal K^0_S mass [12].

B meson candidates are identified using two kinematic variables: beam-energy constrained mass, $M_{\rm bc} = \sqrt{E^2_{\rm beam}/c^4 - |\sum_i \vec{p}_i/c|^2}$, and energy difference, $\Delta E = \sum_i E_i - E_{\rm beam}$, where $E_{\rm beam}$ is the beam energy, and $\vec{p}_i$ and E_i are the momentum and energy, respectively, of the i-th daughter of the reconstructed B candidate in the center-of-mass (CM) frame. We retain events with $5.271\,{\rm GeV}/c^2 < M_{\rm bc} < 5.287\,{\rm GeV}/c^2$ and $-0.10\,{\rm GeV} < \Delta E < 0.15\,{\rm GeV}$ for further analysis. The $M_{\rm bc}$ requirement corresponds to approximately $\pm 3\sigma$ around the nominal B^+ mass [12]. We apply a looser $(-6\sigma, +9\sigma)$ requirement on ΔE as it is used in the fitter (described below). The average number of B candidates found per event is 1.13 (1.49) for $B^+ \to K^0_S K^0_S K^+$ ($K^0_S K^0_S \pi^+$). In events with multiple B candidates, we choose the one with the lowest χ^2 value obtained from a B vertex fit. This criterion selects the correct B-meson candidate in 75% (63%) of MC events for $B^+ \to K^0_S K^0_S K^+$ ($K^0_S K^0_S \pi^+$).

The dominant background is from the $e^+e^- \to q\overline{q}$ ($q = u, d, s, c$) continuum process. To suppress it, observables based on the event shape topology are utilized. The event shape in the CM frame is expected to be spherical for $B\overline{B}$ events, in contrast to jet-like for continuum events. We employ another NN [11] to combine the following six input variables: the Fisher discriminant formed from 16 modified Fox-Wolfram moments [13], the cosine of the angle between the B momentum and the z axis, the cosine of the angle between the B thrust and the z axis, the cosine of the angle between the thrust axis of the B candidate and that of the rest of the event, the ratio of the second to the zeroth order Fox-Wolfram moments, and the vertex separation along the z axis between the B candidate and the remaining tracks. The first five quantities are calculated in the CM frame. The NN training and optimization are performed with signal and $q\overline{q}$ Monte Carlo (MC) simulated events. The signal MC sample is generated with the EvtGen program [14] assuming a three-body phase space. We require the NN output (C_{NB}) to be greater than -0.2 to substantially reduce the continuum background. The relative signal efficiency due to this requirement is approximately 91%, whereas the achieved continuum suppression is close to 84% for both decays. The remainder of the C_{NB} distribution strongly peaks near 1.0 for signal, making it difficult to model it

with an analytic function. However, its transformed variable

$$C'_{NB} = \log\left[\frac{C_{NB} - C_{NB,\min}}{C_{NB,\max} - C_{NB}}\right], \tag{2}$$

where $C_{NB,\min} = -0.2$ and $C_{NB,\max} \simeq 1.0$, has a Gaussian-like distribution.

The background due to B decays mediated via the dominant $b \to c$ transition is studied with an MC sample comprising such decays. The resulting ΔE and $M_{\rm bc}$ distributions are found to strongly peak in the signal region for both $B^+ \to K^0_S K^0_S K^+$ and $K^0_S K^0_S \pi^+$ decays. For $B^+ \to K^0_S K^0_S K^+$, the peaking background predominantly stems from $B^+ \to D^0 K^+$ with $D^0 \to K^0_S K^0_S$ and $B^+ \to \chi_{c0}(1P) K^+$ with $\chi_{c0}(1P) \to K^0_S K^0_S$. To suppress these backgrounds, we exclude candidates for which $M_{K^0_S K^0_S}$ lies in the ranges of $[1.85, 1.88]\,{\rm GeV}/c^2$ and $[3.38, 3.45]\,{\rm GeV}/c^2$ corresponding to about $\pm 3\sigma$ window around the nominal D^0 and $\chi_{c0}(1P)$ mass [12], respectively. On the other hand, in case of $B^+ \to K^0_S K^0_S \pi^+$, the peaking background largely arises from $B^+ \to D^0 \pi^+$ with $D^0 \to K^0_S K^0_S$. To suppress this background, we exclude candidates for which $M_{K^0_S K^0_S}$ lies in the aforementioned D^0 mass window.

There are a few background modes that contribute in the $M_{\rm bc}$ signal region but have the ΔE peak shifted from zero on the positive (negative) side for $B^+ \to K^0_S K^0_S K^+$ ($K^0_S K^0_S \pi^+$). The so-called "feed-across background" modes, mostly arising due to K–π misidentification, are identified with a $B\overline{B}$ MC sample in which one of the B mesons decays via $b \to u, d, s$ transitions. The feed-across background includes contribution from $B \to K^0_S K^0_S \pi$ ($K^0_S K^0_S K$) in $B^+ \to K^0_S K^0_S K^+$ ($K^0_S K^0_S \pi^+$). The events that remain after removing the signal and feed-across components comprise the "combinatorial background." After all selection requirements, the efficiency for correctly reconstructed signal events ($\epsilon_{\rm rec}$) is 24% (28%) for $B^+ \to K^0_S K^0_S K^+$ ($K^0_S K^0_S \pi^+$). The fraction of misreconstructed signal events ($f_{\rm SCF}$) is 0.45% (1.05%) for $B^+ \to K^0_S K^0_S K^+$ ($K^0_S K^0_S \pi^+$). As $f_{\rm SCF}$ represents a small fraction of the signal events for both decays, we consider it as a part of signal. Note that $\epsilon_{\rm rec}$ and $f_{\rm SCF}$ are determined with an MC simulation in which decays are generated assuming a three-body phase space.

The signal yield and $\mathcal{A}_{CP}$ are obtained with an unbinned extended maximum likelihood fit to the two-dimensional distributions of ΔE and C'_{NB}. We define a probability density function (PDF) for each event category j (signal, $q\overline{q}$, combinatorial $B\overline{B}$, and feed-across backgrounds) as

$$\mathcal{P}^i_j \equiv \frac{1}{2}(1 - q^i . \mathcal{A}_{CP,j}) \times \mathcal{P}_j(\Delta E^i) \times \mathcal{P}_j(C'^i_{NB}), \tag{3}$$

where i denotes the event index, q^i is the charge of the B candidate in the event (± 1 for $B^\pm$), $\mathcal{P}_j$ is the PDF corresponding to the component j. Since the correlation between ΔE and C'_{NB} is found to be negligible, the product of two individual PDFs is a good approximation for the total PDF. We apply a tight requirement on $M_{\rm bc}$ instead of including it in the fitter as it exhibits large correlation with ΔE for signal and feed-across components. The extended likelihood function is

$$\mathcal{L} = \frac{e^{-\sum_j n_j}}{N!} \prod_i \Big[\sum_j n_j \mathcal{P}^i_j\Big], \tag{4}$$

where n_j is the yield of the event category j and N is the total number of events. To account for crossfeed between the $B \to K^0_S K^0_S K$ and $B \to K^0_S K^0_S \pi$ channels, they are simultaneously

TABLE I: List of PDFs used to model the ΔE and C'_{NB} distributions for various event categories for $B \to K^0_S K^0_S K$. G, AG, and Poly1 denote Gaussian, asymmetric Gaussian, and first order polynomial, respectively.

Event category	ΔE	C'_{NB}
Signal	3 G+Poly1	G+AG
Continuum $q\overline{q}$	Poly1	2 G
Combinatorial $B\overline{B}$	Poly1	2 G
Feed-across	G+Poly1	G

fitted, with the $B \to K^0_S K^0_S K$ signal yield in the correctly reconstructed sample determining the normalization of the crossfeed in the $B \to K^0_S K^0_S \pi$ fit region, and vice versa.

Table I lists the PDF shapes used to model ΔE and C'_{NB} distributions for various event categories for $B \to K^0_S K^0_S K$. For $B \to K^0_S K^0_S \pi$, we use similar PDF shapes except for the feed-across background component, where we use a sum of a Gaussian, asymmetric Gaussian and first order polynomial to parametrize ΔE, and a sum of Gaussian and asymmetric Gaussian functions to parametrize C'_{NB}. For $B \to K^0_S K^0_S K$, the yields for all event categories except for that of the combinatorial $B\overline{B}$ background are allowed to vary in the fit. The latter yield is fixed to the MC value as it is found to be correlated with the continuum background yield. For $B \to K^0_S K^0_S \pi$, the yields for all event categories are allowed to vary. For both $B \to K^0_S K^0_S K$ and $K^0_S K^0_S \pi$, the following PDF shape parameters of the continuum background are floated: the slope of the first order polynomial used for ΔE, and one of the means and widths of the Gaussian functions used to model C'_{NB}. The PDF shapes for signal and other background components are fixed to the corresponding MC expectations. Shared parameters in the simultaneous fit are the signal yields of $K^0_S K^0_S K$ and $K^0_S K^0_S \pi$. The ratio of the $K^0_S K^0_S K$ feed-across to the signal $K^0_S K^0_S \pi$ yield is floated, whereas the ratio of the $K^0_S K^0_S \pi$ feed-across to the signal $K^0_S K^0_S K$ yield is fixed in the fitter. This is because the latter contribution is small. We correct the signal ΔE and C'_{NB} PDF shapes for possible data-MC differences, according to the values obtained with a large-statistics control sample of $B \to D^0(K^0_S \pi^+\pi^-)\pi$. The same correction factors are also applied for the feed-across background component of $B \to K^0_S K^0_S \pi$. The stability of the two-dimensional simultaneous fit is checked via ensemble tests using both PDF-sampled and simulated MC events.

Figure 2 shows ΔE and C'_{NB} projections of the fit to B^+ and B^- samples separately for $B \to K^0_S K^0_S K$ and overall fit for $B \to K^0_S K^0_S \pi$. We determine the branching fraction as,

$$\mathcal{B}(B^+ \to K^0_S K^0_S h^+) = \frac{N_{\rm sig}}{\epsilon \times N_{B\bar{B}} \times [\mathcal{B}(K^0_S \to \pi\pi)]^2} \tag{5}$$

where, $N_{\rm sig}$, ϵ and $N_{B\bar{B}}$ are the signal yield, corrected reconstruction efficiency and total number of $B\bar{B}$ pairs, respectively. For $B^+ \to K^0_S K^0_S \pi^+$, we obtain a signal yield of 69 ± 26, where the error is statistical only. The inclusive branching fraction for $B^+ \to K^0_S K^0_S \pi^+$ is $(0.70 \pm 0.26 \pm 0.07) \times 10^{-6}$, where the first uncertainty is statistical and the second is systematic. Its signal significance is estimated as $\sqrt{2\log(\mathcal{L}_0/\mathcal{L}_{\rm max})}$, where $\mathcal{L}_0$ and $\mathcal{L}_{\rm max}$ are the likelihood value with the signal yield set to zero and for the nominal case, respectively. Including systematic uncertainties (described below), we determine the significance to be 2.6 standard deviations (σ). In view of the significance being less than 3σ, we set an upper

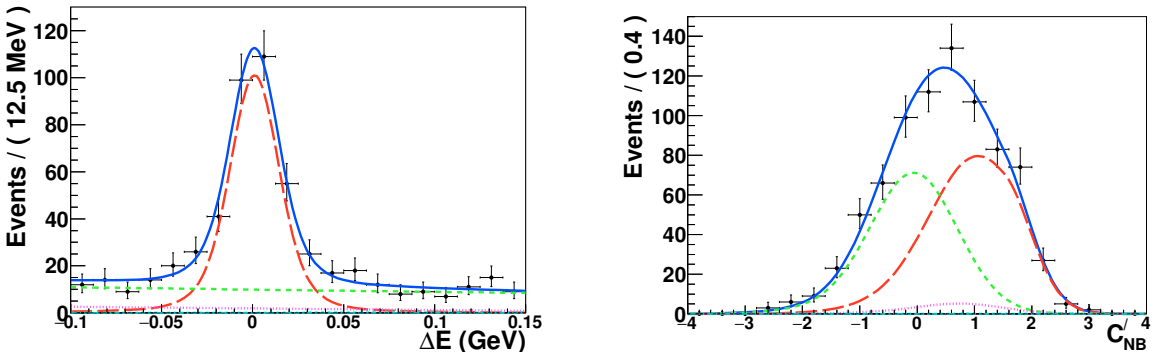

a) $B^+ \to K^0_S K^0_S K^+$

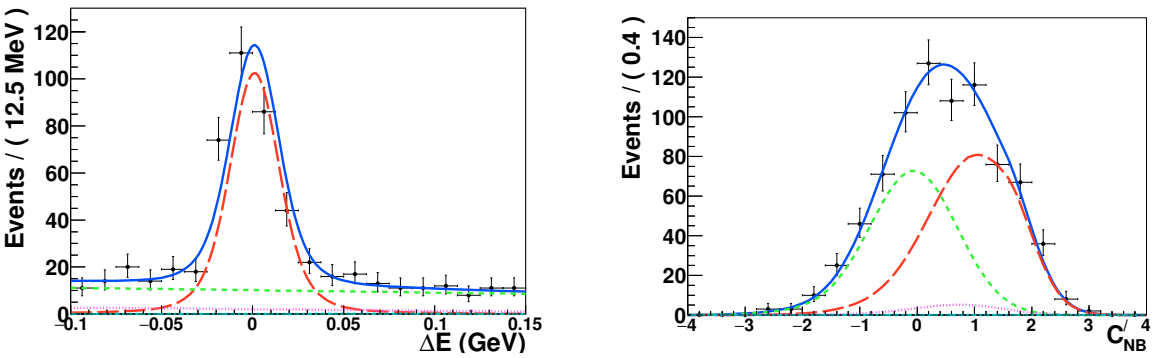

b) $B^- \to K^0_S K^0_S K^-$

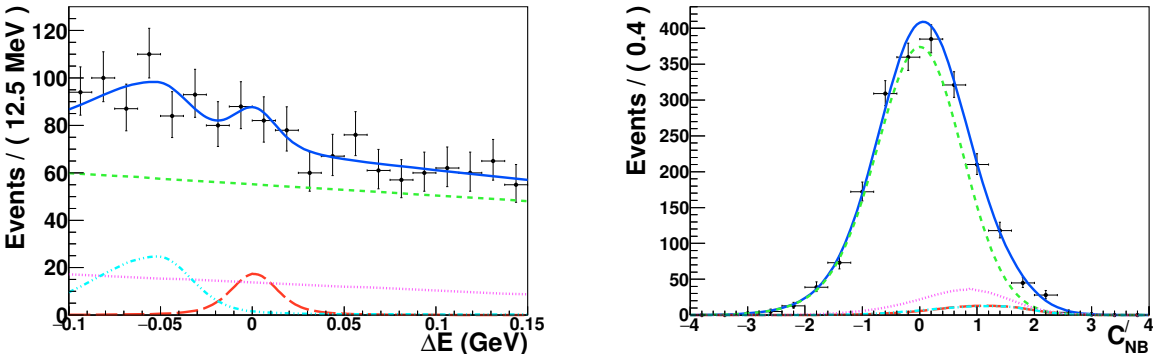

c) $B^\pm \to K^0_S K^0_S \pi^\pm$

FIG. 2: (colour online). Projections of two-dimensional simultaneous fit to ΔE for $C'_{NB} > 0.0$ and C'_{NB} for $|\Delta E| < 50\,\text{MeV}$. Points with error bars are the data, solid blue curves are the total PDF, long dashed red curve is the signal component, dashed green curve is the continuum $q\overline{q}$ background, dotted magenta curve is the combinatorial $B\overline{B}$ background and dash-dotted cyan curve is the feed-across background.

limit (UL) on the branching fraction of $B \to K^0_S K^0_S \pi$. For this purpose we convolve the likelihood with a Gaussian function of width equal to the systematic error. Assuming a flat prior we set an UL of 1.14×10^{-6} at 90% confidence level. Our limit is somewhat looser than that of BaBar [8] owing to our comparatively larger signal yield.

For $B^+ \to K^0_S K^0_S K^+$, we perform the fit in seven bins of $M_{K^0_S K^0_S}$ to incorporate contribu-

tions from possible two-body intermediate resonances. Efficiency, signal yield, differential branching fraction, and $\mathcal{A}_{CP}$ thus obtained are listed in Table II. Figure 3 shows the branching fraction and $\mathcal{A}_{CP}$ plotted as a function of $M_{K^0_S K^0_S}$. We observe an excess of events around $1.5\,\mathrm{GeV}/c^2$, whereas no significant evidence for CP asymmetry is found in any of the bins. The inclusive branching fraction obtained by integrating the differential branching fractions over the entire $M_{K^0_S K^0_S}$ range is

$$\mathcal{B}(B^+ \to K^0_S K^0_S K^+) = (10.64 \pm 0.49 \pm 0.44) \times 10^{-6}, \tag{6}$$

where the first uncertainty is statistical and the second is systematic. Similarly, the inclusive $\mathcal{A}_{CP}$ over the full $M_{K^0_S K^0_S}$ range is

$$\mathcal{A}_{CP}(B \to K^0_S K^0_S K) = (-0.6 \pm 3.9 \pm 3.4)\%. \tag{7}$$

This is obtained by weighting the $\mathcal{A}_{CP}$ value in each bin with the fitted yield divided by the detection efficiency in that bin. As the statistical uncertainties are bin-independent, their total contribution is a quadratic sum. On the other hand, for the systematic uncertainties, the total contribution from the bin-correlated sources is taken as a linear sum while that from the bin-uncorrelated sources is determined as a quadratic sum. The results are in agreement with BaBar [6], where they had reported an overall $\mathcal{A}_{CP}$ consistent with zero, and the presence of intermediate resonances $f_0(1500)$ and $f'_2(1525)$ in the aforementioned invariant-mass region.

TABLE II: Signal yield, efficiency, differential branching fraction, and $\mathcal{A}_{CP}$ for each $M_{K^0_S K^0_S}$ bins.

$M_{K^0_S K^0_S}$ (GeV/c^2)	Yield	Eff. (%)	$\Delta\mathcal{B} \times 10^{-6}$	A$_{CP}$ (%)
<1.1	98 ± 11	24.0 ± 0.4	$1.14 \pm 0.13 \pm 0.06$	$-3.2 \pm 11.0 \pm 3.0$
1.1-1.3	145 ± 14	23.4 ± 0.2	$1.74 \pm 0.17 \pm 0.07$	$-4.4 \pm 9.1 \pm 3.1$
1.3-1.6	250 ± 18	22.9 ± 0.1	$3.06 \pm 0.23 \pm 0.12$	$+6.1 \pm 6.8 \pm 3.6$
1.6-2.0	122 ± 13	21.8 ± 0.1	$1.56 \pm 0.17 \pm 0.06$	$+16.0 \pm 10.0 \pm 4.0$
2.0-2.3	103 ± 12	24.1 ± 0.1	$1.20 \pm 0.14 \pm 0.05$	$-1.8 \pm 11.0 \pm 2.9$
2.3-2.7	92 ± 12	25.2 ± 0.1	$1.02 \pm 0.13 \pm 0.04$	$-2.0 \pm 12.0 \pm 3.2$
> 2.7	86 ± 15	26.3 ± 0.0	$0.91 \pm 0.16 \pm 0.04$	$-31.2 \pm 17.0 \pm 4.2$

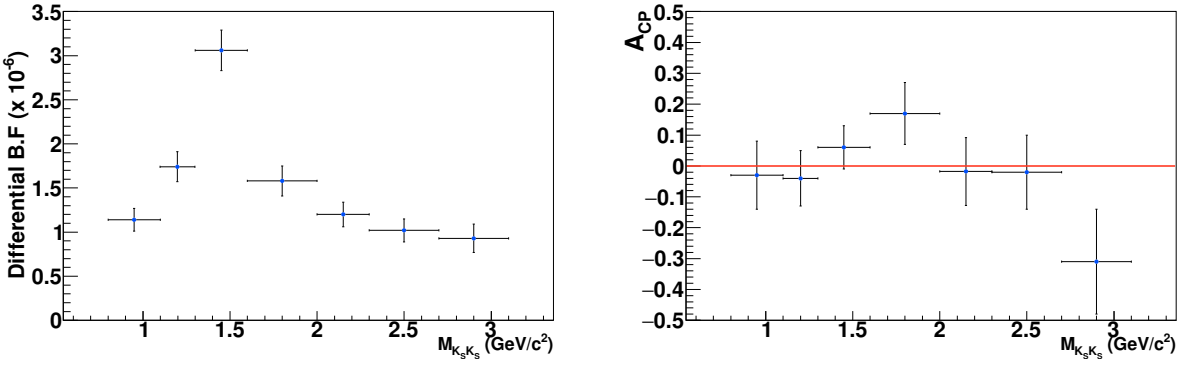

FIG. 3: Differential branching fraction (left) and $\mathcal{A}_{CP}$ (right) for $B^+ \to K^0_S K^0_S K^+$ as a function of $M_{K^0_S K^0_S}$. The horizontal red line indicates null *CP* asymmetry.

Major sources of systematic uncertainties on the branching fractions are same for both $B^+ \to K^0_S K^0_S K^+$ and $K^0_S K^0_S \pi^+$ decays. These are listed along with their contributions in Tables III and IV. We use partially reconstructed $D^{*+} \to D^0(K^0_S\pi^+\pi^-)\pi^+$ decays to assign the systematic uncertainty due to charged-track reconstruction (0.35% per track). The $D^{*+} \to D^0(K^-\pi^+)\pi^+$ control sample is used to determine the systematic uncertainty due to the $R_{K/\pi}$ requirement. The uncertainty due to the total number of $B\bar{B}$ pairs is 1.37%. The uncertainties due to the $M_{\rm bc}$ and continuum suppression criteria are estimated using a control sample of $B^+ \to D^0(K^0_S\pi^-\pi^+)\pi^+$ decays. The uncertainty arising due to the $K^0_S \to \pi^+\pi^-$ reconstruction is estimated from $D^0 \to K^0_S K^0_S$ analysis [15]. Potential fit bias is checked by performing an ensemble test comprising 1000 pseudo-experiments, where the signal component is embedded from the corresponding MC samples and PDF shapes are used to generate the dataset for other event categories. The uncertainties due to signal PDF shape parameters are estimated by varying the correction factors (discussed earlier) by $\pm 1\sigma$ of their error. Similarly, the uncertainties due to background PDF shape parameters are calculated by varying all fixed parameters by $\pm 1\sigma$. We evaluate the uncertainty due to the fixed yields of combinatorial backgrounds by varying it up and down by its statistical error. The uncertainties due to the dependence of PDF shapes on $M_{K^0_S K^0_S}$ are evaluated in each $M_{K^0_S K^0_S}$ bin and propagated to the branching fraction measurement. The total systematic uncertainty is calculated by summing all these contributions in quadrature.

TABLE III: Systematic uncertainties in the branching fraction for $B \to K^0_S K^0_S \pi$.

Source	Relative uncertainty in $\mathcal{B}$ (%)
Tracking	0.35
Particle identification	0.80
Number of $B\overline{B}$ pairs	1.37
Continuum suppression	0.34
Requirement on $M_{\rm bc}$	0.03
K^0_S reconstruction efficiency	3.25
Fit bias	1.86
Signal PDF	$+2.50, -0.00$
Combinatorial $B\bar{B}$ PDF	$+2.42, -1.78$
Feed-across PDF	$+6.47, -9.56$
Fixed yields	0.00

Systematic uncertainties on $\mathcal{A}_{CP}$ are listed in Table IV. The systematic errors due to the signal and background modeling are estimated with the same procedure as done for the branching fraction. Uncertainties due to intrinsic detector bias on charged particle detection is evaluated from the $\mathcal{A}_{CP}$ value obtained using a data sample of $89.4\,\text{fb}^{-1}$ recorded 60 MeV below the $\Upsilon(4S)$ resonance. We obtain an asymmetry of $(-2.7 \pm 2.0)\%$ for this dataset, from which we take the absolute value of the central shift (2.7%) as the uncertainty due to detector asymmetry. The uncertainties due to the dependence of PDF shapes on $M_{K^0_S K^0_S}$ are evaluated in each $M_{K^0_S K^0_S}$ bin and propagated to the $\mathcal{A}_{CP}$ value.

TABLE IV: Systematic uncertainties for the branching fraction and $\mathcal{A}_{CP}$ in the individual bins for $B \to K^0_S K^0_S K$. "†" indicates the uncertainty is $M_{K^0_S K^0_S}$ dependent and an ellipsis indicates a value below 0.05% (0.001) in $\mathcal{B}$ ($\mathcal{A}_{CP}$).

Source	Relative uncertainty in $\mathcal{B}$ (%)						
$M_{K^0_S K^0_S}$(GeV/c^2)	<1.1	$1.1-1.3$	$1.3-1.6$	$1.6-2.0$	$2.0-2.3$	$2.3-2.7$	>2.7
Tracking			0.35				
Particle identification			0.80				
Number of $B\overline{B}$ pairs			1.37				
Continuum suppression			0.34				
Requirement on $M_{\rm bc}$			0.03				
K^0_S reconstruction efficiency			3.22				
Fit bias			0.59				
Signal and background PDF†	...	$^{+0.00}_{-0.69}$	$^{+0.00}_{-0.57}$	$^{+0.81}_{-0.81}$	$^{+0.00}_{-0.97}$	$^{+0.00}_{-1.09}$	$^{+1.16}_{-1.16}$
Fixed yields†	...	...	...	...	...	...	...
PDF dependence on $M^{\dagger}_{K^0_S K^0_S}$	4.08	0.35	0.60	0.41	0.95	0.00	1.75

Source	Absolute uncertainties in $\mathcal{A}_{CP}$						
$M_{K^0_S K^0_S}$(GeV/c^2)	<1.1	$1.1-1.3$	$1.3-1.6$	$1.6-2.0$	$2.0-2.3$	$2.3-2.7$	>2.7
Signal and background PDF†	$^{-0.000}_{+0.005}$	$^{-0.000}_{+0.005}$	$^{-0.003}_{+0.000}$	$^{-0.031}_{+0.000}$	$^{-0.000}_{+0.006}$	$^{-0.000}_{+0.002}$	$^{-0.001}_{+0.006}$
Fixed yields†	...	...	...	...	...	...	...
PDF dependence on $M^{\dagger}_{K^0_S K^0_S}$	0.003	0.004	0.009	0.010	0.002	0.005	0.015
Detector bias			0.027				

In summary, we have reported measurements of the suppressed decays $B^+ \to K^0_S K^0_S K^+$ and $B^+ \to K^0_S K^0_S \pi^+$ using the full $\Upsilon(4S)$ data sample collected with the Belle detector. We perform a two-dimensional simultaneous fit to extract the signal yields of both decays. We report a 90% upper limit on the branching fraction of 1.14×10^{-6} for the decay $B^+ \to K^0_S K^0_S \pi^+$. We also report the branching fraction and $\mathcal{A}_{CP}$ as a function of $M_{K^0_S K^0_S}$ for $B^+ \to K^0_S K^0_S K^+$. We observe an excess of events at low $M_{K^0_S K^0_S}$ region, likely caused by the two-body intermediate resonances reported by BaBar [6]. An amplitude analysis with more data is needed to further elucidate the nature of these resonances. The measured inclusive branching fraction and direct *CP* asymmetry are $\mathcal{B}(B^+ \to K^0_S K^0_S K^+) = (10.64 \pm 0.49 \pm 0.44) \times 10^{-6}$ and $\mathcal{A}_{CP} = (-0.6 \pm 3.9 \pm 3.4)\%$, respectively. These supersede Belle's earlier measurements [7] and constitute the most precise results to date.

[1] A. Bevan *et al.* Eur. Phys. J. C **74**, 3026 (2014).
[2] R. Aaij *et al.* (LHCb Collaboration), Phys. Rev. D **90**, 112004 (2014).
[3] R. Aaij *et al.* (LHCb Collaboration), Phys. Rev. L **112**, 011801 (2014).
[4] C.-L. Hsu *et al.* (Belle Collaboration), Phys. Rev. D **96**, 031101(R) (2017).
[5] Inclusion of charge-conjugate reactions are implicit unless stated otherwise.
[6] J.P. Lees *et al.* (BaBar Collaboration), Phys. Rev. D **85**, 112010 (2012).
[7] A. Garmash *et al.* (Belle Collaboration), Phys. Rev. D **69**, 012001 (2004).
[8] B. Aubert *et al.* (BaBar Collaboration), Phys. Rev. D **79**, 051101(R) (2009).
[9] A. Abashian *et al.* (Belle Collaboration), Nucl. Instrum. Methods Phys. Res., Sect. A **479**, 117 (2002); also see the detector section in J. Brodzicka *et al.*, Prog. Theor. Exp. Phys. (2012) 04D001.
[10] S. Kurokawa and E. Kikutani, Nucl. Instrum. Methods Phys. Res., Sect. A **499**, 1 (2003), and other papers included in this Volume; T. Abe *et al.*, Prog. Theor. Exp. Phys. (2013) 03A001 and following articles up to 03A011.
[11] M. Feindt and U. Kerzel, Nucl. Instrum. Methods Phys. Res., Sect. A **559**, 190 (2006).
[12] M. Tanabashi *et al.* (Particle Data Group), Phys. Rev. D **98**, 030001 (2018).
[13] S. H. Lee *et al.* (Belle Collaboration), Phys. Rev. Lett. **91**, 261801 (2003).
[14] D. J. Lange, Nucl. Instrum. Methods Phys. Res., Sect. A **462**, 152 (2001).
[15] N. Dash *et al.* (Belle Collaboration), Phys. Rev. Lett **119**, 171801 (2017).